

# High Rates of Quinone-Alkyne Cycloaddition Reactions are Dictated by Entropic Factors

Johannes A. M. Damen,<sup>[a]</sup> Jorge Escorihuela,<sup>[b]</sup> Han Zuilhof,<sup>[a, c, d]</sup> Floris L. van Delft,<sup>[a, e]</sup> and Bauke Albada<sup>\*[a]</sup>

**Abstract:** Reaction rates of strained cycloalkynes and cycloalkenes with 1,2-quinone were quantified by stopped flow UV-Vis spectroscopy and computational analysis. We found that the strained alkyne BCN–OH **3** ( $k_2$  1824 M<sup>-1</sup>s<sup>-1</sup>) reacts > 150 times faster than the strained alkene TCO–OH **5** ( $k_2$  11.56 M<sup>-1</sup>s<sup>-1</sup>), and that derivatization with a carbamate can lead to a reduction of the rate constant with almost half. Also, the 8-membered strained alkyne BCN–OH **3** reacts 16 times faster than the more strained 7-membered THS **2** ( $k_2$  110.6 M<sup>-1</sup>s<sup>-1</sup>). Using the linearized Eyring equation we determined the thermodynamic activation parameters of these two strained alkynes, revealing that the SPOCQ reaction

of quinone **1** with THS **2** is associated with  $\Delta H^\ddagger$  of 0.80 kcal/mol,  $\Delta S^\ddagger = -46.8$  cal/K·mol, and  $\Delta G^\ddagger = 14.8$  kcal/mol (at 25 °C), whereas the same reaction with BCN–OH **3** is associated with,  $\Delta H^\ddagger = 2.25$  kcal/mol,  $\Delta S^\ddagger = -36.3$  cal/K·mol, and  $\Delta G^\ddagger = 13.1$  kcal/mol (at 25 °C). Computational analysis supported the values obtained by the stopped-flow measurements, with calculated  $\Delta G^\ddagger$  of 15.6 kcal/mol (in H<sub>2</sub>O) for the SPOCQ reaction with THS **2**, and with  $\Delta G^\ddagger$  of 14.7 kcal/mol (in H<sub>2</sub>O) for the SPOCQ reaction with BCN–OH **3**. With these empirically determined thermodynamic parameters, we set an important step towards a more fundamental understanding of this set of rapid click reactions.

## Introduction

The strain-promoted oxidation-controlled *ortho*-quinone (SPOCQ) cycloaddition is an oxidation-inducible [4 + 2] cycloaddition of a 1,2-quinone with a strained cyclic alkyne or alkene that follows an inverse electron-demand Diels-Alder (IEDDA)

mechanism.<sup>[1,2]</sup> Due to its high rates and efficiency, SPOCQ chemistry has been successfully employed for the chemical modification of surfaces and for the preparation of bioconjugates.<sup>[3–6]</sup> In comparison to the widely applied strain-promoted azide-alkyne cycloaddition (SPAAC), SPOCQ benefits from reaction rates that are orders of magnitude higher and provides the option of spatiotemporal control by in situ generation of the *o*-quinone from phenols, including biogenic versions utilizing exposed tyrosine residues on proteins.<sup>[7–11]</sup> Whereas details of the mechanism and rate constants of SPAAC are well-established,<sup>[12,13]</sup> in-depth investigations into SPOCQ are scarce and mostly limited to computational studies.<sup>[14]</sup>

In the current paper, the experimental determination of second-order rate constants and a computational analysis of SPOCQ between a model *o*-quinone and various strained alkenes and alkynes is described. We determined thermodynamic activation parameters of the reaction with strained alkynes, and correlation to high-level computational analysis provided quantitative insight in the dominant forces driving the conversion, which surprisingly contradict earlier deduced explanations.<sup>[15,16]</sup> We also quantified the effect of derivatization of two of the most commonly employed strained unsaturated systems, BCN (*endo*-bicyclo[6.1.0]non-4-yne) and TCO (*trans*-cyclooctene), on the associated second-order rate constants to translate our findings to derivatives used in conjugation chemistry. Lastly, we report an improved synthesis of THS (compound **2** in Scheme 1; 3,3,6,6-tetramethyl-1-thiacycloheptyne sulfoximide, see Supporting Information).<sup>[17–22]</sup>

[a] J. A. M. Damen, Prof. Dr. H. Zuilhof, Prof. Dr. F. L. van Delft, Dr. B. Albada  
Laboratory of Organic Chemistry  
Wageningen University & Research  
Stippeneng 4, Wageningen, 6807 WE (the Netherlands)  
E-mail: bauke.albada@wur.nl  
Homepage: www.orc.wur.nl

[b] Dr. J. Escorihuela  
Departamento de Química Orgánica  
Universitat de València  
Avda. Vicent Andrés Estellés s/n  
València, Burjassot, 46100 (Spain)

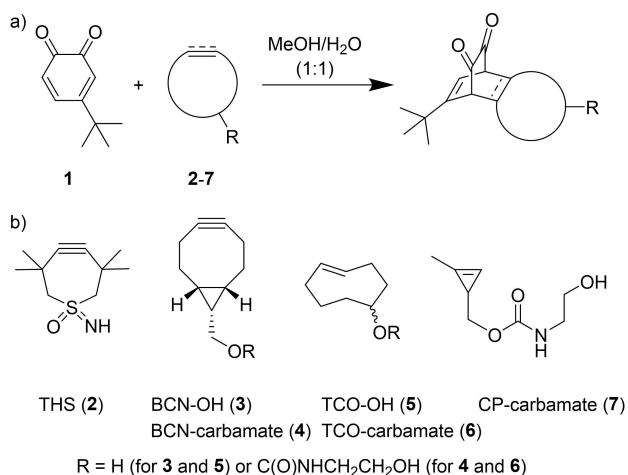
[c] Prof. Dr. H. Zuilhof  
School of Pharmaceutical Sciences and Technology  
Tianjin University  
Tianjin, 300072 (China)

[d] Prof. Dr. H. Zuilhof  
Department of Chemical and Materials Engineering  
Faculty of Engineering  
King Abdulaziz University  
Jeddah, 21589 (Saudi Arabia)

[e] Prof. Dr. F. L. van Delft  
Synaffix BV  
Industrielaan 63, Oss, 5349 AE (the Netherlands)

Supporting information for this article is available on the WWW under <https://doi.org/10.1002/chem.202300231>

© 2023 The Authors. Chemistry - A European Journal published by Wiley-VCH GmbH. This is an open access article under the terms of the Creative Commons Attribution License, which permits use, distribution and reproduction in any medium, provided the original work is properly cited.



**Scheme 1.** (a) Generalized scheme for the SPOCQ reaction. (b) Matrix of strained unsaturated carbon-carbon bond containing reagents that were studied.

## Results and Discussion

Single crystals of THS (2) suitable for X-ray crystallography were grown from chloroform/pentane via the vapor diffusion method, resulting in the crystal structure of this alkyne (Figure 1). The structure revealed that the single bonds to the alkyne triple bond are bent at 151° angles on either side in a coplanar fashion (torsion angle of only 0.2°). The C≡C bond length is 1.191 Å, and the alkyne is slightly bent out of plane at a 12° angle versus the backbone carbon atoms formed by the two sp<sup>3</sup> hybridized carbon atoms between the alkyne and sulfoximide. The propargylic C—C≡C bonds are both 1.48 Å long and are thereby considerably shorter than the other C—C bonds

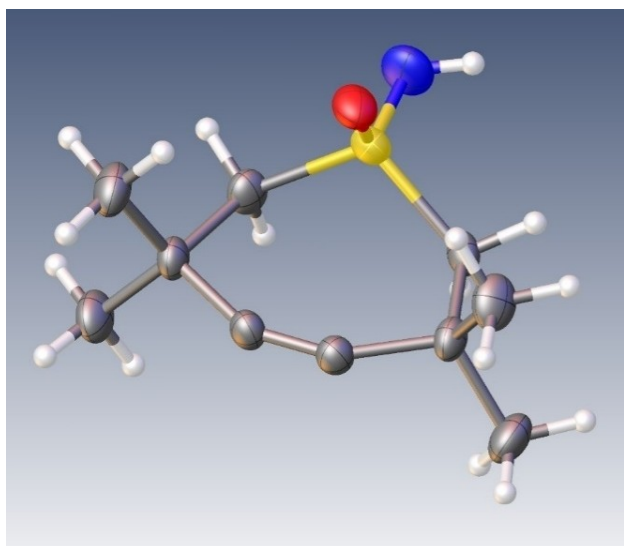


**Figure 1.** Molecular structure of THS (2) according to X-ray structure determination. ORTEP depicted with thermal ellipsoids drawn at 50% probability level.

in the molecule ranging from 1.53–1.55 Å. The C—S bonds are elongated to 1.81 Å and the sulfur atom lies at a 76° torsion angle above the plane of the ring. Lastly, the oxygen atom is positioned as the axial substituent (S=O 1.466 Å) and the imine as the equatorial substituent (S=NH 1.516 Å).

The model SPOCQ reaction we investigated is depicted in Scheme 1a. Specifically, we employed the relatively stable 4-*tert*-butyl-*ortho*-quinone 1, which has a distinct optical absorption maximum at 395 nm that allows an easy spectroscopic analysis of the reaction rates. Our matrix of unsaturated carbon-carbon bond-containing compounds 2–7 covers a range of ring sizes, associated strain and relevant derivatization (Scheme 1b).

Firstly, we compared the recently published THS 2 – a highly strained 7-membered cyclic alkyne with unprecedented reaction rate constants in SPAAC reactions with azides<sup>[22,23]</sup> – with BCN–OH 3, an 8-membered cyclic alkyne that is currently one of the benchmark reagents for metal-free click chemistry applications.<sup>[24]</sup> [Of note: DBCO, by far the most frequently employed cyclooctyne for SPAAC reactions, was found not to display significant reactivity in SPOCQ and was therefore omitted from the matrix.<sup>[11]</sup>] In addition, we applied two strained alkenes that are commonly used in tetrazine ligations,<sup>[25,26]</sup> i.e. 8-membered diastereomeric TCO–OH 5 (and its carbamate 6) as well as a derivative of the 3-membered cyclopropene (CP) carbamate 7; this compound was used in functionalized form due to instability of the parent alcohol.<sup>[27–29]</sup> Importantly, as all of these strained unsaturated systems are usually not applied as such, but incorporated into a functionalized construct, we also determined the effect of alcohol carbamoylation on the rate constants of BCN and TCO (with compounds 4 and 6), respectively.

Accurate determination of the reaction rates and second-order rate constants of the SPOCQ reaction was performed by stopped-flow UV-Vis spectroscopic analysis at 25 °C in a methanol-water (1:1) mixture (for set-up see Supporting Information).<sup>[30]</sup> Pseudo-first-order reaction conditions in which 10–100-fold excess of the strained systems 2–7 with respect to *o*-quinone 1 were used. The concentration-independent second-order rate constant  $k_2$  was derived from the slope of the  $k'$  (or  $k_{\text{obs}}$ ) versus  $[B]_0$ -plot (with  $[B]_0$  equaling the starting concentration of the excess reagent, Figure 2). Notably, the SPOCQ rate constant for BCN–OH 3 of 1824 ( $\pm 16$ ) M<sup>−1</sup>s<sup>−1</sup> is substantially higher than previously reported values (496–1112 M<sup>−1</sup>s<sup>−1</sup>),<sup>[1,7]</sup> which may be rationalized by the fact that sub-optimal conditions were employed previously (e.g., close to equimolar ratios, suboptimal mixing, inability to measure conversion within seconds after mixing). Secondly, we surprisingly found that the  $k_2$  value for THS 2 of 110.6 ( $\pm 2.3$ ) M<sup>−1</sup>s<sup>−1</sup> is approximately 16 times lower than that of BCN–OH 3, which is in striking contrast with the reported observation that THS 2 reacts at least 5 times faster than BCN–OH 3 in cycloaddition with azide (i.e., SPAAC).<sup>[22]</sup>

In line with our earlier observations, strained alkenes undergo slower cycloaddition with *o*-quinone than strained alkynes. Specifically, TCO–OH 5 with a  $k_2$  value of 11.56 ( $\pm 0.11$ ) M<sup>−1</sup>s<sup>−1</sup> is 10-fold less reactive than THS 2 and 160-fold compared to BCN–OH 3. With respect to the influence of chemical derivatiza-

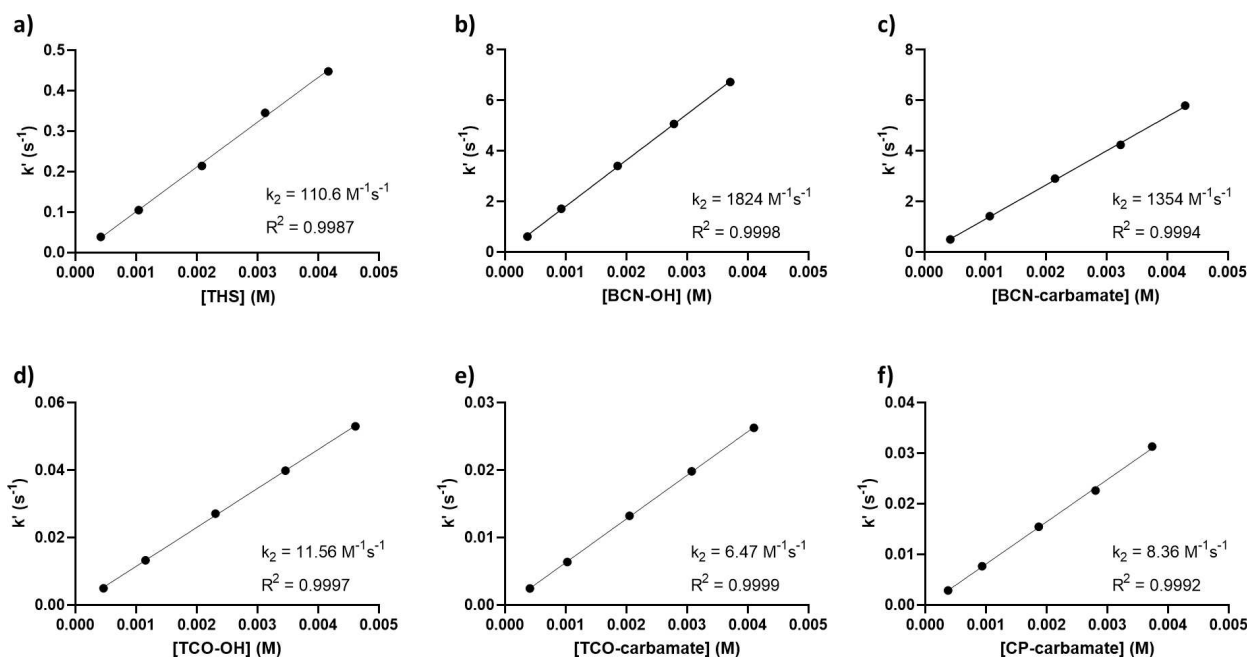


**Figure 2.**  $k_2$ -plots for the SPOCQ reactions of 2–7 determined at 25 °C in MeOH/H<sub>2</sub>O (1:1) for: (a) THS 2, (b) BCN–OH 3, (c) BCN-carbamate 4, (d) TCO-OH 5, (e) TCO-carbamate 6, (f) methylcyclopropene (CP) carbamate 7.

tion, conversion of the hydroxyl group of the well-established probes BCN and TCO into a carbamate lowered the rate slightly (26–44%), i.e., to 1354 ( $\pm 19$ ) M<sup>-1</sup>s<sup>-1</sup> for BCN-carbamate 4, and to 6.47 ( $\pm 0.04$ ) M<sup>-1</sup>s<sup>-1</sup> for TCO-carbamate 6. Surprisingly, the  $k_2$  value of 8.36 ( $\pm 0.14$ ) M<sup>-1</sup>s<sup>-1</sup> for cyclopropene-derived probe 7 is somewhat higher than that of TCO-carbamate 6, suggesting that cyclopropene derivatives are potentially a preferred class of strained alkenes for application in SPOCQ chemistry, specifically when a small ring size is preferred, such as in crowded environments.<sup>[4]</sup>

The unexpected rate difference between THS 2 and BCN–OH 3 was dissected by determining thermodynamic activation parameters obtained from the linearized Eyring equation (Eq. (1), see Supporting Information).<sup>[31–34]</sup> To this end, the  $k_2$  values were determined at 5, 13, 21, 29 and 37 °C, respectively (Figure 3). This range was chosen as the lower temperatures represents values used for the preparation of protein conjugates such as ADCs, while the highest temperature is relevant for potential in vivo applications. As a result, the reaction of *o*-quinone 1 with THS 2 is associated with a  $\Delta H^\ddagger$  of 0.80 kcal/mol,  $\Delta S^\ddagger = -46.8$  cal/K·mol, and  $\Delta G^\ddagger = 14.8$  kcal/mol (at 25 °C). Similarly, for reaction of 1 with BCN–OH 3,  $\Delta H^\ddagger = 2.25$  kcal/mol,  $\Delta S^\ddagger = -36.3$  cal/K·mol, and  $\Delta G^\ddagger = 13.1$  kcal/mol (at 25 °C).

Clearly, the enthalpy required to form the TS for the reaction between 1 and either BCN–OH 3 or THS 2 is only minimal. Considering that the kinetic energy  $kT$  at room temperature translates to 0.6 kcal/mol, we found thermodynamic parameters that will aid in the interpretation of the contributions of any secondary orbital interactions that were recently proposed for the SPOCQ reaction between BCN–OH 3

and *o*-quinone 1.<sup>[15,16]</sup> The investigated SPOCQ reactions are by and large entropy-controlled reactions. Specifically, the large negative  $\Delta S^\ddagger$  values prove that both reactions are associative in nature and require precise positioning of the reagents to form the transition states. In addition, more order needs to be imposed on the reaction of THS 2 than on that of BCN–OH 3 (in other words, BCN 3 is intrinsically more preorganized towards the TS than THS 2), which we tentatively explain by considering that the TS formed during approach of THS 2 to the plane of 1 has to accommodate the steric bulk of the four methyl groups next to the alkyne. This difference in entropy at 25 °C between 2 and 3 (difference in  $T\Delta S^\ddagger = 3.2$  kcal/mol) outcompetes the difference in enthalpic factors ( $-1.5$  kcal/mol) to yield an overall difference in Gibbs energy of activation at 25 °C of 1.7 kcal/mol in the advantage of BCN–OH 3 SPOCQ over THS 2 SPOCQ.

To further support our empirical findings, computational investigations on the TS were performed using the M06-2X functional with the 6-311+G(d,p) basis set and including the implicit solvent model SMD.<sup>[35]</sup> To this end, the free energy barriers for the cycloaddition of the minimal reactive warheads of TCO, *endo*-BCN, THS, and CP were calculated for the reaction in water and in MeOH. The transition state structures and the calculated activation free energies ( $\Delta G^\ddagger$ ), activation free enthalpies ( $\Delta H^\ddagger$ ), and reaction free energies ( $\Delta G_{\text{RXN}}$ ) are displayed in Figure 4. As observed, the activation free energies for these SPOCQ reactions range from 15 to 20 kcal/mol, in reasonable agreement with experiment, given the non-explicit nature of our solvent model. In all cases, the reaction proceeds via a non-synchronous transition state with C–C distances ranging from 2.11 to 2.46 Å. In agreement with experimental results, the computed energies predict that BCN will react appreciably faster

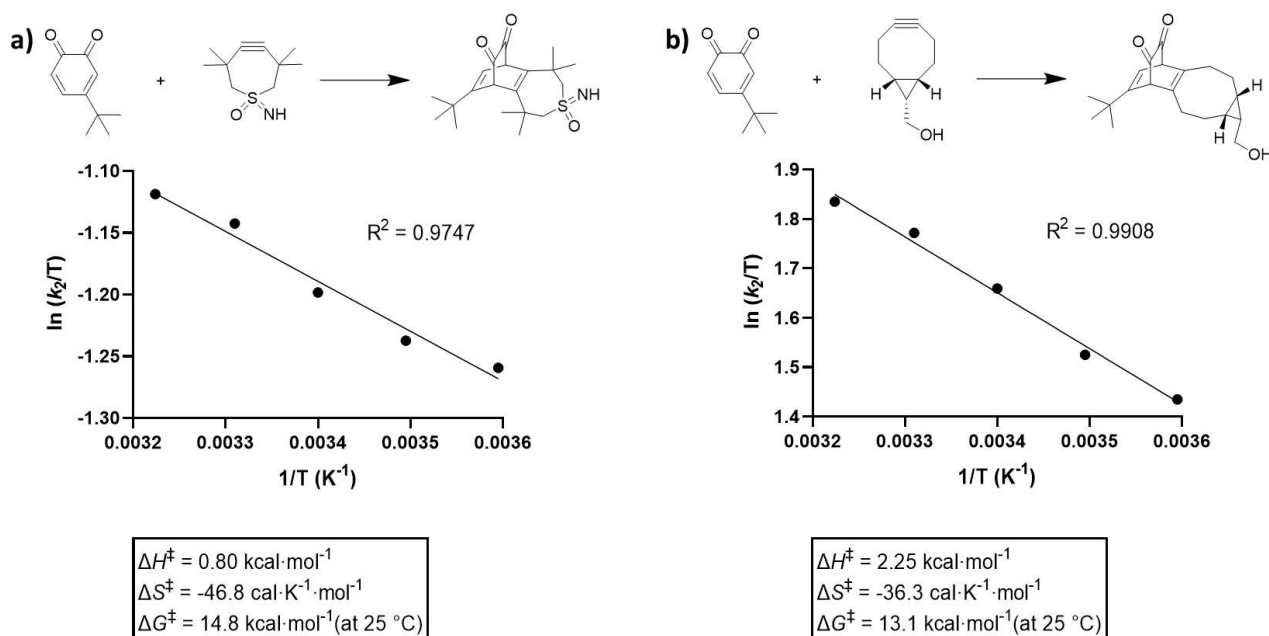


Figure 3. Eyring plots of the reaction of quinone 1 with (a) THS 2 or (b) BCN-OH 3.

with *o*-quinone 1 than THS and TCO, with a factor 4 and 50 times, respectively.

## Conclusions

In conclusion, our improved synthesis of THS (2) resulted in sufficient material for single crystal X-ray diffraction analysis, showing bond angles of 151° for the sp-hybridized carbon atoms. Stopped-flow UV-Vis spectroscopic analysis of the cycloaddition of 4-*tert*-butyl-*ortho*-quinone 1 first of all revealed that the novel strained alkyne THS 2 reacts 16 times slower than BCN-OH 3 in SPOCQ. Also, we find that derivatization of the strained warhead reduces this rate slightly. Most importantly, experimentally quantified thermodynamic activation parameters showed that the reaction of THS 2 and BCN-OH 3 with *o*-quinone 1 is essentially an entropy-controlled reaction.

## Experimental Section

(3,3,6,6-tetramethylthiepane-4,5-diylidene)bis(hydrazine) was synthesised according to classic literature procedures. 4-*tert*-butyl-*ortho*-quinone 1 was synthesised by the method described by Borrmann.<sup>[5,6]</sup> Methylcyclopropene-ethanolamine-carbamate (CP-carb) 7 was synthesised according to literature procedures. *Trans*-cyclooct-4-enol (TCO-OH) 5 was purchased as a mixture of diastereomers from BroadPharm (San Diego, CA, United States), its carbamate derivative 6 was prepared according to literature procedure.<sup>[36]</sup> *Endo*-bicyclo[6.1.0]non-4-yn-9-ol (BCN-OH) 3 was kindly donated by Synaffix (Oss, The Netherlands).

## Synthesis of THS 2

A 250 mL round-bottom flask was charged with (3,3,6,6-tetramethylthiepane-4,5-diylidene)bis(hydrazine) (878.1 mg; 3.84 mmol; 1 eq), ammonium carbonate (1.55 g; 16.1 mmol; 4.2 eq), iodobenzene diacetate (5.09 g; 15.8 mmol; 4.1 eq) and a magnetic stirring bar. The solid reagents were dry mixed in the flask affording a homogeneous powder mixture. The flask was then precooled in an ice-water bath for 15 min. Upon stirring, 45 mL precooled methanol (at 0°C) was added to the flask at once. The reaction mixture immediately turned yellow and gasses evolved. The neck of the flask was fitted with a septum including a bleed needle. The yellow colour disappears within ten minutes. The reaction mixture was left to stir in an ice/water bath at 0°C for 3.5 h and formation of the target compound could be monitored with TLC ( $R_f = 0.18$  in EtOAc). The solvent was then removed in vacuo. The residue was taken up in 100 mL DCM and was washed twice with 50 mL demineralized water. The target compound was re-extracted twice from the combined aqueous phases using 50 mL DCM. The combined organic phases were dried over Na<sub>2</sub>SO<sub>4</sub> and filtered over a folding filter into a 250 mL round-bottom flask. Solvent was removed in vacuo. Target product was purified by Flash chromatography (dry packed on silica with DCM; eluent: isocratic EtOAc). This afforded 184 mg of THS as colourless needle crystals. Yield 24%. <sup>1</sup>H NMR (700 MHz, CDCl<sub>3</sub>) δ 3.24 (d,  $J = 14.1$  Hz, 2H), 3.15 (d,  $J = 14.1$  Hz, 2H), 1.43 (s, 6H), 1.27 (s, 6H). <sup>13</sup>C NMR (176 MHz, CDCl<sub>3</sub>) δ 101.6, 71.2, 34.8, 27.7, 26.7. HRMS (ESI) calc. for C<sub>10</sub>H<sub>18</sub>NOS [M+H]<sup>+</sup> 200.1104; found 200.1105. Single crystals were grown suitable for X-ray crystallography analysis. The structure can be retrieved from the Cambridge Crystallographic Data Centre (CCDC deposition number 2249007).

## Synthesis of BCN-carbamate 4

A scintillation vial was charged with *endo*-BCN-OH 3 (100.2 mg; 0.67 mmol; 1 eq), a magnetic stirring bar and the contents were then dissolved in 3 mL MeCN. *N,N'*-disuccinimidyl carbonate

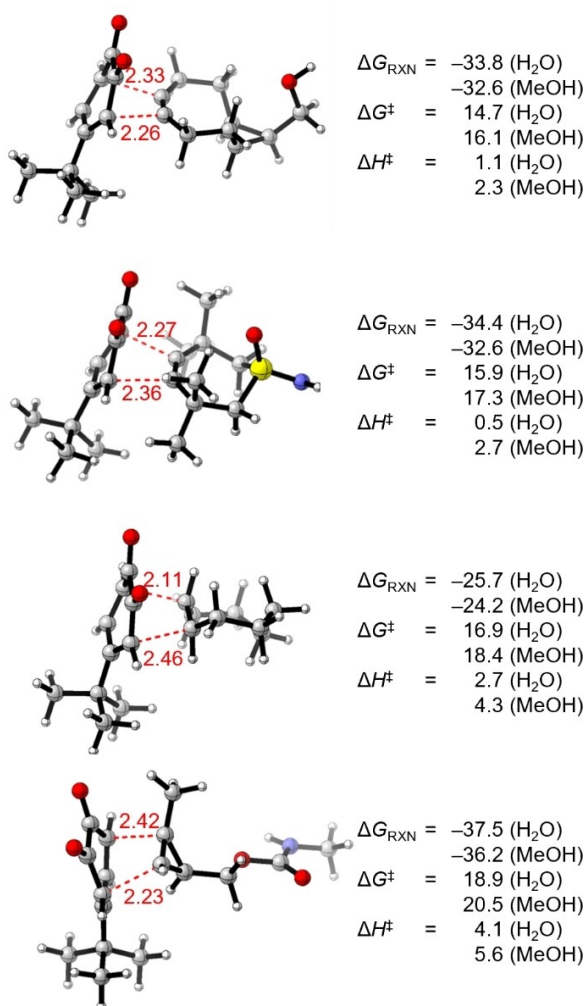


**Figure 4.** Transition state structures with associated Gibbs free energies of reaction, Gibbs activation free energies, and enthalpy of activation for the SPOCQ of BCN, THS, TCO and CP (top to bottom), with quinone 1 in the two solvents that were used in the experiment. Bond lengths are shown in red in Å and energies and enthalpies are given in kcal/mol.

(264.5 mg; 1 mmol; 1.5 eq) and triethylamine (276  $\mu$ L; 2 mmol; 3 eq) were added to the reaction mixture under magnetic stirring. The homogenous reaction mixture was stirred for 1.5 hr, after which TLC indicated complete formation of BCN succinimidyl carbonate ( $R_f=0.6$  in EtOAc/PE 1:1;  $R_f=0.44$  for BCN-OH). Then, ethanolamine (200  $\mu$ L; 3.3 mmol; 5 eq) was added to the reaction mixture, which turned into a very turbid dispersion. According to TLC the reaction was complete within 15 min ( $R_f=0.17$  in EtOAc/PE 1:1). The reaction mixture was taken up in 10 mL demineralized water and 20 mL EtOAc, which was subsequently extracted. The aqueous phase was reextracted with 10 mL EtOAc. The combined organic phases were washed with 10 mL demineralized water, dried over Na<sub>2</sub>SO<sub>4</sub>, filtered, and solvent was removed in vacuo. The crude product was then purified by flash chromatography, eluent: 50% EtOAc/hexane (isocratic). This afforded 123.9 mg of target compound *endo*-BCN-carb **4** as a clear viscous oil. Yield 78%. <sup>1</sup>H NMR (700 MHz, CDCl<sub>3</sub>)  $\delta$  5.17 (s, 1H), 4.14 (d,  $J=8.1$  Hz, 2H), 3.71 (t,  $J=5.1$  Hz, 2H), 3.34 (q,  $J=5.4$  Hz, 2H), 2.51 (bs, 1H), 2.33–2.15 (m, 6H), 1.61–1.52 (m, 2H), 1.39–1.30 (m, 1H), 1.24 (s, 1H), 0.98–0.89 (m, 2H). <sup>13</sup>C NMR (176 MHz, CDCl<sub>3</sub>)  $\delta$  157.7, 98.9, 63.2, 62.5, 43.5, 29.1, 21.5,

20.2, 17.8. HRMS (ESI) calc. for C<sub>13</sub>H<sub>19</sub>NO<sub>3</sub>Na [M+Na]<sup>+</sup> 260.1257; found 260.1258.

### Stopped-flow kinetic studies

The reaction of 4-*tert*-butyl-ortho-quinone **1** with probes **2–7** was measured under pseudo-first order conditions in 1:1 MeOH/MilliQ water following the decay of the specific absorption band at 395 nm for *o*-quinone **1**. Two respective equimolar solutions of *o*-quinone **1** and the probe of interest were loaded into the two separate driver syringes of the RX2000 Rapid Kinetics Spectrometer Accessory (Applied Photophysics). The accessory is attached to a thermostat bath and to a Cary 60 UV-Vis spectrophotometer. The solutions in the driver syringes were thermostatted for at least 15 min prior to measurement. Upon measurement, the contents of the two driver syringes were flown simultaneously through the cuvette and measurement starts upon abruptly stopping the flow. Single wavelength measurements were then recorded every 12.5 ms at 395 nm. The measurements were performed in quadruplicate until the signal stabilises. This setup utilises equal volumes of the reagents, thereby halving each respective concentration in the cuvette.

The experiments were conducted using 40  $\mu$ M solutions of *o*-quinone **1** (1 eq) and 0.4–4 mM solutions of probe (i.e., 10–100 eq) to allow for acquisition of sufficient data points for analysis. From these,  $k_2$  plots were determined at 25 °C with the varying stoichiometry of the target probes. Eyring plots were determined at a set stoichiometry of 1:10 at varying temperatures of 5, 13, 21, 29, 37 °C. Data analysis was then performed in GraphPad Prism 9 Version 9.3.1 (471) by exponential one phase decay fitting using nonlinear regression until a plateau of constant value is reached, leading to an observed pseudo-first-order rate constant  $k'$  (see Supporting Information for additional details).

### Computational Analysis

All DFT calculations were performed using Gaussian16 Rev.B01.<sup>[35]</sup> The Minnesota functional M06-2X with the 6-31G(d) basis was used for geometry optimization of minima and transition states. A frequency analysis was performed using the same level of theory to confirm the presence of a minima with no imaginary frequency or a transition state with a single imaginary frequency. Next, single point energy calculations were performed at the M06-2X with the augmented 6-311++G(d,p) basis set including the solvent with a polarizable continuum model (PCM) using the M06-2X/6-31G(d) optimized geometries. Gibbs free energies were calculated by applying thermal corrections of the M06-2X/6-31G(d) frequency analysis to M06-2X/6-311++G(d,p)//M06-2X/6-31G(d) electronic energies. Intrinsic reaction coordinate (IRC) calculations were performed to verify the expected connections of the first-order saddle points with the local minima found on the potential energy surface.

### Associated Content

**Supporting Information.** Additional details on the synthesis of the various compounds, the setup used for the stopped-flow experiments, data on all kinetic measurements, derivatization of mathematical equations and specifics of the computational studies. This material is available free of charge via the Internet at <http://pubs.acs.org>.

## Funding Sources

This work is funded by the NWO Gravity Program Institute for Chemical Immunology (ICI), project number ICI00027.

## Abbreviations

BCN	<i>endo</i> -bicyclo[6.1.0]non-4-yne
CP	cyclopropene
IEDDA	inverse electron-demand Diels–Alder
SPAAC	strain-promoted alkyne-azide cycloaddition
SPOCQ	strain-promoted oxidation-induced <i>o</i> -quinone
TCO	( <i>trans</i> -cyclooctene)
THS	3,3,6,6-tetramethyl-7-thiacycloheptane sulfoximine
TS	transition state

## Acknowledgements

We thank Gabriele Kociok-Köhn (University of Bath, UK) for her work on obtaining and processing of the single crystal X-ray structure, and Yifei Zhou for his assistance in generating the image shown in Figure 1.

## Conflict of Interests

The authors declare no conflict of interest.

## Data Availability Statement

The data that support the findings of this study are available in the supplementary material of this article.

**Keywords:** eyring plot · secondary orbital interactions · SPOCQ · thermodynamic reaction parameters · TMTHSI

- J. Escorihuela, A. Das, W. J. E. Looijen, F. L. Van Delft, A. J. A. Aquino, H. Lischka, H. Zuilhof, *J. Org. Chem.* **2018**, *83*, 244.
- B. Albada, J. F. Keijzer, H. Zuilhof, F. van Delft, *Chem. Rev.* **2021**, *121*, 7032.
- R. Sen, J. Escorihuela, F. van Delft, H. Zuilhof, *Angew. Chem. Int. Ed.* **2017**, *56*, 3299.
- D. Gahtory, R. Sen, A. R. Kuzmyn, J. Escorihuela, H. Zuilhof, *Angew. Chem. Int. Ed.* **2018**, *57*, 10118.
- A. Borrmann, O. Fatunsin, J. Dommerholt, A. M. Jonker, D. W. P. M. Löwik, J. C. M. Van Hest, F. L. Van Delft, *Bioconjugate Chem.* **2015**, *26*, 257.
- J. J. Bruins, B. Albada, F. Van Delft, *Chem. Eur. J.* **2018**, *24*, 4749.
- J. J. Bruins, D. Blanco-Ania, V. Van Der Doef, F. L. Van Delft, *Chem. Commun.* **2018**, *54*, 7338.
- J. J. Bruins, A. H. Westphal, B. Albada, K. Wagner, L. Bartels, H. Spits, W. J. H. Van Berkel, F. L. Van Delft, *Bioconjugate Chem.* **2017**, *28*, 1189.
- J. J. Bruins, C. Van de Wouw, J. F. Keijzer, B. Albada, F. L. van Delft, in *Enzyme-Mediated Ligation Methods*, (Eds. T. Nuijens, M. Schmidt), Springer New York, **2019**; pp. 357–368.
- J. J. Bruins, C. Van de Wouw, K. Wagner, L. Bartels, B. Albada, F. L. Van Delft, *ACS Omega.* **2019**, *4*, 11801.
- J. J. Bruins, J. A. M. Damen, M. A. Wijdeven, L. P. W. M. Lelieveldt, F. L. Van Delft, B. Albada, *Bioconjugate Chem.* **2021**, *32*, 2167.
- J. Dommerholt, O. Van Rooijen, A. Borrmann, C. F. Guerra, F. M. Bickelhaupt, F. L. Van Delft, *Nat. Commun.* **2014**, *5*, 5378.
- S. L. Scinto, D. A. Bilodeau, R. Hincapie, W. Lee, S. S. Nguyen, M. Xu, C. W. am Ende, M. G. Finn, K. Lang, Q. Lin, J. P. Pezacki, J. A. Prescher, *Nat. Rev. Methods Primers* **2021**, *1*, 30.
- J. Escorihuela, W. J. E. Looijen, X. Wang, A. J. A. Aquino, H. Lischka, H. Zuilhof, *J. Org. Chem.* **2020**, *85*, 13557.
- B. J. Levandowski, D. Svatunek, B. Sohr, H. Mikula, K. N. Houk, *J. Am. Chem. Soc.* **2019**, *141*, 2224.
- B. J. Levandowski, D. Svatunek, B. Sohr, H. Mikula, K. N. Houk, *J. Am. Chem. Soc.* **2019**, *141*, 18641.
- B. Verbelen, E. Siemes, A. Ehnbohm, C. Räuber, K. Rissanen, D. Wöll, C. Bolm, *Org. Lett.* **2019**, *21*, 4293.
- J.-F. Lohier, T. Glachet, H. Marzag, A.-C. Gaumont, V. Reboul, *Chem. Commun.* **2017**, *53*, 2064.
- A. Krebs, H. Kimling, *Tetrahedron Lett.* **1970**, *11*, 761.
- G. De Almeida, E. M. Sletten, H. Nakamura, K. K. Palaniappan, C. R. Bertozzi, *Angew. Chem. Int. Ed.* **2012**, *51*, 2443.
- M. King, R. Baati, A. Wagner, *Chem. Commun.* **2012**, *48*, 9308.
- J. Weterings, C. J. F. Rijcken, H. Veldhuis, T. Meulemans, D. Hadavi, M. Timmers, M. Honing, H. Ippel, R. M. J. Liskamp, *Chem. Sci.* **2020**, *11*, 9011.
- E. R. Hebels, F. Bindt, J. Walther, M. Van Geijn, J. Weterings, Q. Hu, C. Colombo, R. Liskamp, C. Rijcken, W. E. Hennink, T. Vermondan, *Biomacromolecules* **2022**, ASAP, Doi: <https://doi.org/10.1021/acs.biomac.2c00865>.
- J. Dommerholt, S. Schmidt, R. Temming, L. J. A. Hendriks, F. P. J. T. Rutjes, J. C. M. Van Hest, D. J. Lefeber, P. Friedl, F. L. Van Delft, *Angew. Chem. Int. Ed.* **2010**, *49*, 9422.
- B. L. Oliveira, Z. Guo, G. J. L. Bernardes, *Chem. Soc. Rev.* **2017**, *46*, 4895.
- M. Baalman, L. Neises, S. Bitsch, H. Schneider, L. Deweid, P. Werther, N. Ilkenhans, M. Wolfring, M. J. Ziegler, J. Wilhelm, H. Kolmar, R. A. Wombacher, *Angew. Chem. Int. Ed.* **2020**, *59*, 12885.
- D. M. Patterson, L. A. Nazarova, B. Xie, D. N. Kamber, J. A. Prescher, *J. Am. Chem. Soc.* **2012**, *134*, 18638.
- J. Yang, J. Šečkute, C. M. Cole, N. K. Devaraj, *Angew. Chem. Int. Ed.* **2012**, *51*, 7476.
- F. L. Carter, V. L. Frampton, *Chem. Rev.* **1964**, *64*, 497.
- M. Wang, D. Svatunek, K. Rohlfing, Y. Liu, H. Wang, B. Giglio, H. Yuan, Z. Wu, Z. Li, J. Fox, *Theranostics.* **2016**, *6*, 887.
- K. J. Laidler, M. C. King, *J. Phys. Chem.* **1983**, *87*, 2657.
- H. Eyring, *J. Chem. Phys.* **1935**, *3*, 107.
- M. G. Evans, M. Polanyi, *Trans. Faraday Soc.* **1935**, *31*, 875.
- W. F. K. Wynne-Jones, H. Eyring, *J. Chem. Phys.* **1935**, *3*, 492.
- M. J. Frisch, G. W. Trucks, H. B. Schlegel, G. E. Scuseria, M. A. Robb, J. R. Cheeseman, G. Scalmani, V. Barone, G. A. Petersson, H. Nakatsuji, X. Li, M. Caricato, A. V. Marenich, J. Bloino, B. G. Janesko, R. Gomperts, B. Mennucci, H. P. Hratchian, J. V. Ortiz, A. F. Izmaylov, J. L. Sonnenberg, D. Williams-Young, F. Ding, F. Lipparini, F. Egidi, J. Goings, B. Peng, A. Petrone, T. Henderson, D. Ranasinghe, V. G. Zakrzewski, J. Gao, N. Rega, G. Zheng, W. Liang, M. Hada, M. Ehara, K. Toyota, R. Fukuda, J. Hasegawa, M. Ishida, T. Nakajima, Y. Honda, O. Kitao, H. Nakai, T. Vreven, K. Throssell, J. A. Montgomery Jr., J. E. Peralta, F. Ogliaro, M. J. Bearpark, J. J. Heyd, E. N. Brothers, K. N. Kudin, V. N. Staroverov, T. A. Keith, R. Kobayashi, J. Normand, K. Raghavachari, A. P. Rendell, J. C. Burant, S. S. Iyengar, J. Tomasi, M. Cossi, J. M. Millam, M. Klene, C. Adamo, R. Cammi, J. W. Ochterski, R. L. Martin, K. Morokuma, O. Farkas, J. B. Foresman, D. J. Fox, M. J. Frisch, *Gaussian 16*, Revision B.01, Gaussian, Inc.: Wallingford CT, **2016**.
- D. Liang, K. Wu, R. Tei, T. W. Bumpus, J. Ye, J. M. Baskin, *Proc. Natl. Acad. Sci. USA* **2019**, *116*, 15453–15462.

Manuscript received: January 23, 2023

Accepted manuscript online: March 21, 2023

Version of record online: May 31, 2023